

# Bayesian photometric redshift estimation

Narciso Benítez

Astronomy Department, UC Berkeley, 601 Campbell Hall, Berkeley, CA

## ABSTRACT

Photometric redshift estimation is becoming an increasingly important technique, although the currently existing methods present several shortcomings which hinder their application. Here it is shown that most of those drawbacks are efficiently eliminated when Bayesian probability is consistently applied to this problem. The use of prior probabilities and Bayesian marginalization allows the inclusion of valuable information, e.g. the redshift distributions or the galaxy type mix, which is often ignored by other methods. It is possible to quantify the accuracy of the redshift estimation in a way with no equivalents in other statistical approaches; this property permits the selection of galaxy samples for which the redshift estimation is extremely reliable. In those cases when the *a priori* information is insufficient, it is shown how to ‘calibrate’ the prior distributions, using even the data under consideration.

There is an excellent agreement between the  $\sim 100$  HDF spectroscopic redshifts and the predictions of the method, with a rms error  $\Delta z/(1+z_{spec}) = 0.08$  up to  $z < 6$  and no systematic biases nor outliers. Note that these results have not been reached by minimizing the difference between spectroscopic and photometric redshifts (as is the case with empirical training set techniques), which may lead to an overestimation of the accuracy. The reliability of the method is further tested by restricting the color information to the UBV filters. The results thus obtained are shown to be more reliable than those of standard techniques even when the latter include near-IR colors.

The Bayesian formalism developed here can be generalized to deal with a wide range of problems which make use of photometric redshifts. Several applications are outlined, e.g. the estimation of individual galaxy characteristics as the metallicity, dust content, etc., or the study of galaxy evolution and the cosmological parameters from large multicolor surveys. Finally, using Bayesian probability it is possible to develop an integrated statistical method for cluster mass reconstruction which simultaneously considers the information provided by gravitational lensing and photometric redshift estimation.

*Subject headings:* photometric redshifts; galaxy evolution; statistical methods; gravitational lensing

## 1. Introduction

The advent of the new class of 10-m ground based telescopes is having a strong impact on the study of galaxy evolution. For instance, instruments as LRIS at the Keck allow observers to regularly secure redshifts for dozens of  $I \approx 24$  galaxies in several hours of exposure. Technical advances in the instrumentation, combined with the proliferation of similar telescopes in the next years guarantees a vast increase in the number of galaxies, bright and faint, for which spectroscopical redshifts will be obtained in the near future. Notwithstanding this progress in the sheer numbers of available spectra, the  $I \approx 24$  ‘barrier’ (for reasonably complete samples) is likely to stand for a time, as there are not foreseeable dramatic improvements in the telescope area or detection techniques.

Despite the recent spectacular findings of very high redshift galaxies, (Dey et al. 1998, Franx et al. 1997, Frye, Broadhurst & Benítez 1998), it is extremely difficult to secure redshifts for such objects. On the other hand, even moderately deep ground based imaging routinely contain many high redshift galaxies (although hidden amongst myriads of foreground ones), not to mention the Hubble Deep Field or the images that will be available with the upcoming Advanced Camera. To push further in redshift the study of galaxy evolution is therefore very important to develop techniques able to extract galaxy redshifts from multicolor photometry data.

This paper applies the methods of Bayesian probability theory to photometric redshift estimation. Despite the efforts of Thomas Loredo, who has written stimulating reviews on the subject (Loredo 1990, 1992), Bayesian methods are still far from being one of the staple statistical techniques in Astrophysics. Most courses and monographs on Statistics only include a small section on Bayes’ theorem, and perhaps as a consequence of that, Bayesian techniques are frequently used *ad hoc*, as another tool from the available panoply of statistical methods. However, as any reader of the fundamental treatise by E.T. Jaynes (1998) can learn, Bayesian probability theory represents an unified look to probability and statistics, which does not intend to complement, but to fully substitute the traditional, ‘frequentist’ statistical techniques (see also Bretthorst 1988, 1990)

One of the fundamental differences between ‘orthodox’ statistics and Bayesian theory, is that the probability is not defined as a frequency of occurrence, but as a reasonable degree of belief. Bayesian probability theory is developed as a rigorous full-fledged alternative to traditional probability and statistics based on this definition and three *desiderata*: a)Degrees of belief should be represented by real numbers, b)One should reason consistently, and c)The theory should reduce to Aristotelian logic when the truth values of hypothesis are known.

One of the most attractive features of Bayesian inference lies on its simplicity. There are two basic rules to manipulate probability, the product rule

$$P(A, B|C) = P(A|C)P(B|A, C) \quad (1)$$

and the sum rule

$$P(A + B|C) = P(A|C) + P(B|C) - P(A, B|C) \quad (2)$$

where “ $A, B$ ” means “ $A$  and  $B$  are true”, and “ $A + B$ ” means “either  $A$  or  $B$  or both are true”. From the product rule, and taking into account that the propositions “ $A, B$ ” and “ $B, A$ ” are identical, it is straightforward to derive Bayes’ theorem

$$P(A|B, C) = \frac{P(A|C)P(B|A, C)}{P(B|C)} \quad (3)$$

If the set of proposals  $B = \{B_i\}$  are mutually exclusive and exhaustive, using the sum rule one can write

$$P(A, B|C) = P(A, \{B_i\}|C) = \sum_i P(A, B_i|C) \quad (4)$$

which is known as Bayesian marginalization. These are the basic tools of Bayesian inference. Properly used and combined with the rules to assign prior probabilities, they are in principle enough to solve most statistical problems.

There are several differences between the methodology presented in this paper and that of Kodama, Bell & Bower 1998, the most significant being the treatment of priors (see Sec. 4). The procedures developed here offer a major improvement in the redshift estimation and based on them it is possible to generate new statistical methods for applications which make use of photometric redshifts (Sec. 6).

The outlay of the paper is the following: Sec. 2 reviews the current methods of photometric redshifts estimation making emphasis on their main sources of error. Sec. 3 introduces an expression for the redshift likelihood slightly different from the one used by other groups when applying the SED-fitting technique. In Sec. 4 it is described in detail how to apply Bayesian probability to photometric redshift estimation; the resulting method is called BPZ. Sec 5 compares the performance of traditional statistical techniques, as maximum likelihood, with BPZ by applying both methods to the HDF spectroscopic sample and to a simulated catalog. Sec. 6 briefly describes how BPZ may be developed to deal with problems in galaxy evolution and cosmology which make use of photometric redshifts. Sec 7 briefly summarizes the main conclusions of the paper.

## 2. Photometric redshifts: training set vs. SED fitting methods

There are two basic approaches to photometric redshift estimation. Using the terminology of Yee 1998, they may be termed ‘SED fitting’ and ‘empirical training set’ methods. The first technique (Koo 1985, Lanzetta, Yahil & Fernández-Soto 1996, Gwyn & Hartwick 1996, Pelló et al. 1996, Sawicki, Lin, & Yee 1997, etc.) involves compiling a library of template spectra, empirical or generated with population synthesis techniques. These templates, after being redshifted and corrected for intergalactic extinction, are compared with the galaxy colors to determine the redshift  $z$  which best fits the observations. The training set technique (Brunner et al. 1997, Connolly et al. 1995, Wang, Bahcall & Turner 1998) starts with a multicolor galaxy sample with apparent magnitudes  $m_0$  and colors  $C$  which has been spectroscopically identified. Using this sample, a relationship of the kind  $z = z(C, m)$  is determined using a multiparametric fit.

It should be said that these two methods are more similar than what it is usually considered. To understand this, let’s analyze how the empirical training set method works. For simplicity, let’s forget about the magnitude dependence and let’s suppose that only two colors  $C = (C_1, C_2)$  are enough to estimate the photometric redshifts, that is, given a set of spectroscopic redshifts  $\{z_{spec}\}$  and colors  $\{C\}$ , the training set method tries to fit a surface  $z = z(C)$  to the data. It must be realized that this method makes a very strong assumption, namely that the surface  $z = z(C)$  is a *function* defined on the color space: each value of  $C$  is assigned one and only one redshift. Visually this means that the surface  $z = z(C)$  does not ‘bend’ over itself in the redshift direction. Although this functionality of the redshift/color relationship cannot be taken for granted in the general case (at faint magnitudes there are numerous examples of galaxies with very similar colors but totally different redshifts), it seems to be a good approximation to the real picture at  $z < 1$  redshifts and bright magnitudes (Brunner et al. 1997). A certain scatter around this surface is allowed: galaxies with the same value of  $(C)$  may have slightly different redshifts and it seems to be assumed implicitly that this scatter is what limits the accuracy of the method.

The SED fitting method is based on the color/redshift relationships generated by each of the library templates  $T$ ,  $C_T = C_T(z)$ . A galaxy at the position  $C$  is assigned the redshift corresponding to the closest point of any of the  $C_T$  curves in the color space. If these  $C_T$  functions are inverted, one ends up with the curves  $z_T = z_T(C_T)$ , which, in general, are not functions; they may present self-crossings (and of course they may also cross each other). If we limit ourselves to the region in the color/redshift space in which the training set method defines the surface  $z = z(C)$ , for a realistic template set the curves  $z_T = z_T(C_T)$  would be embedded in the surface  $z = z(C)$ , conforming its ‘skeleton’ and defining its main features.

The fact that the surface  $z = z(C)$  is continuous, whereas the template-defined curves are sparsely distributed, does not have a great practical difference. The gaps may be filled by finely interpolating between the templates (Sawicki, Lin, & Yee 1997), but this is not strictly necessary: usually the statistical procedure employed to search for the best redshift performs its own interpolation between templates. When the colors of a galaxy do not exactly coincide with one of the templates,  $\chi^2$  or the maximum likelihood method will assign the redshift corresponding to the nearest template in the color space. This is equivalent to the curves  $z_T = z_T(C_T)$  having extended ‘influence areas’ around them, which conform a sort of step-like surface which interpolates across the gaps, and also extends beyond the region limited by them in the color space. Therefore, the SED-fitting method comes with a built-in interpolation (and extrapolation) procedure. For this reason, the accuracy of the photometric redshifts does not change dramatically when using a sparse template set as the one of Coleman, Wu, & Weedman 1980 (Lanzetta, Yahil & Fernández-Soto 1996) or a fine grid of template spectra (Sawicki, Lin, & Yee 1997). The most crucial factor is that the template library, even if it contains few spectra, adequately reflects the main features of real galaxy spectra and therefore the main ‘geographical accidents’ of the surface  $z = z(C)$

The intrinsic similarity between both photometric redshift methods explains their comparable performance, especially at  $z \lesssim 1$  redshift (Hogg et al. 1998). When the topology of the color–redshift relationship is simple, as apparently happens at low redshift, the training set method will probably work slightly better than the template fitting procedure, if only because it avoids the possible systematics due to mismatches between the predicted template colors and the real ones, and also partially because it includes not only the colors of the galaxies, but also their magnitudes, what helps to break the color/redshift degeneracies (see below). However, it must be kept in mind that although the fits to the spectroscopic redshifts give only a dispersion  $\delta z \approx 0.06$  (Connolly et al. 1997), there is not a strong guarantee that the predictive capabilities of the training set method will keep such an accuracy, even within the same magnitude and redshift ranges. As a matter of fact, they do not seem to work spectacularly better than the SED fitting techniques (Hogg et al. 1998), even at low and intermediate redshifts.

However, the main drawback of the training set method is that, due to its empirical and *ad hoc* basis, in principle it can only be reliably extended as far as the spectroscopic redshift limit. Because of this, it may represent a cheaper method of obtaining redshifts than the spectrograph, but which cannot really go much fainter than it. Besides it is difficult to transfer the information obtained with a given set of filters, to another survey which uses a different set. Such an extrapolation has to be done with the help of templates, what makes the method lose its empirical purity. And last but not least, it is obvious that as one goes to higher redshifts/fainter magnitudes the topology of the color-redshift distribution

$z = z(C, m_0)$  displays several nasty degeneracies, even if the near-IR information is included, and it is impossible to fit a single functional form to the color-redshift relationship.

Although the SED fitting method is not affected by some of these limitations, it also comes with its own set of problems. Several authors have analyzed in detail the main sources of errors affecting this method (Sawicki, Lin, & Yee 1997, Fernández-Soto, Lanzetta & Yahil 1998). These errors may be divided into two broad classes:

### 2.1. Color/redshift degeneracies

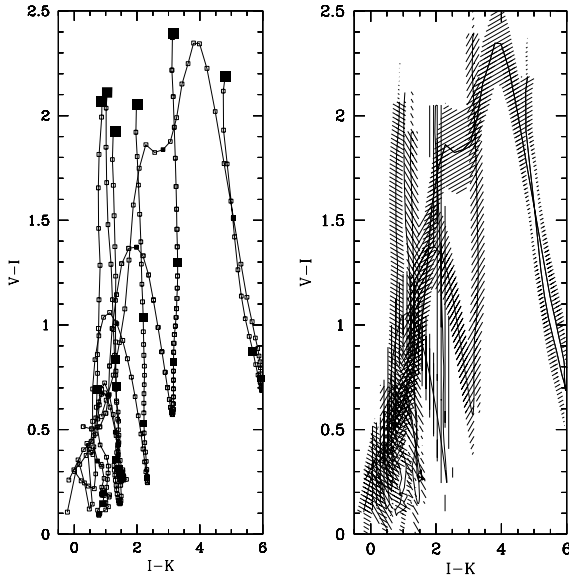


Fig. 1.— a) On the left,  $VI$  vs.  $IK$  for the templates used in Sec 5 in the interval  $1 < z < 5$ . The size of the filled squares grows with redshift, from  $z = 1$  to  $z = 5$ . If these were the only colors used for the redshift estimation every crossing of the lines would correspond to a color/redshift degeneracy. b) To the right, the same color–color relationships ‘thickened’ by a 0.2 photometric error. The probability of color/redshift degeneracies highly increases.

Fig. 1a. shows  $VI$  vs  $IK$  for the morphological types employed in Sec 5 and  $0 < z < 5$ . The color/redshift degeneracies happen when the line corresponding to a single template intersects itself or when two lines cross each other at points corresponding to different redshifts for each of them (these cases correspond to “bendings” in the redshift/color relationship  $z = z(C)$ ). It is obvious that the likelihood of such crossings increases with the extension of the considered redshift range and the number of templates included.

It may seem that even considering a very extended redshift range, such confusions could in principle be easily avoided by using enough filters. However, the presence of color/redshift degeneracies is highly increased by random photometric errors, which can be visualized as a blurring or thickening of the  $C_T(z_T)$  relationship (fig. 1b): each point of the curves in fig. 1a is expanded into a square of size  $\delta C$ , the error in the measured color. The first consequence of this is a ‘continuous’ ( $\delta z \approx \frac{\partial C}{\partial z} \delta C$ ) increase in the rms of the ‘small-scale’ errors in the redshift estimation, and, what is worse, the overlaps in the color-color space become more frequent, with the corresponding rise in the number of ‘catastrophic’ redshift errors. In addition, multicolor information may often be degenerate, so increasing the number of filters does not break the degeneracies; for instance, by applying a simple PCA analysis to the photometric data of the HDF spectroscopic sample it can be shown that the information contained in the seven  $UBVIJHK$  filters for the HDF galaxies can be condensed using only three parameters, the coefficients of the principal components of the flux vectors (see also Connolly et al. 1995). Therefore, if the photometric errors are large, it is not always possible to get totally rid of the degeneracies even increasing the number of filters. This means that the presence of color/redshift degeneracies is unavoidable for faint galaxy samples. The training set method somehow alleviates this problem by introducing an additional parameter in the estimation, the magnitude, which in some cases may break the degeneracy. However, it is obvious that color/redshift degeneracies also affect galaxies with the same magnitude, and the training set method does not even contemplate the possibility of their existence!

The SED-fitting method at least allows for the existence of this problem, although it is not extremely efficient in dealing with it, especially with noisy data. Its choice of redshift is exclusively based on the goodness of fit between the observed colors and the templates. In cases as the one described above, where two or more redshift/morphological type combinations have practically the same colors, the value of the likelihood  $\mathcal{L}$  would have two or more approximately equally high maxima at different redshifts (see fig. 2). Depending on the random photometric error, one maximum would prevail over the others, and a small change in the flux could involve a catastrophic change in the estimated redshift (see fig. 2). However, in many cases there is additional information, discarded by ML, which could potentially help to solve such conundrums. For instance, it may be known from previous experience that one of the possible redshift/type combinations is much more likely than any other given the galaxy magnitude, angular size, shape, etc. In that case, and since the likelihoods are not informative enough, it seems clear that the more reasonable decision would be to choose the option which is more likely *a priori* as the best estimate. Plain common sense dictates that one should compare all the possible hypotheses with the data, as ML does, but simultaneously keeping in mind the degrees of plausibility assigned

to them by previous experience. There is not a simple way of doing this within ML, at best one may remove or change the redshift of the problematic objects by hand or devise *ad hoc* solutions for each case. In contrast, Bayesian probability theory allows to include this additional information in a rigorous and consistent way, effectively dealing with this kind of errors (see Sec 4)

## 2.2. Template incompleteness

In some cases, the spectra of observed galaxies have no close equivalents in the template library. Such galaxies will be assigned the redshift corresponding to the nearest template in the color/redshift space, no matter how distant from the observed color it is in absolute terms. The solution is obvious, one has to include enough templates in the library so that all the possible galaxy types are considered. As was explained above, the SED fitting techniques perform their own ‘automatic’ interpolation and extrapolation, so once the main spectral types are included in the template library, the results are not greatly affected if one finely interpolates among the main spectra. The effects of using a correct but incomplete set of spectra are shown in Sec 5.

Both sources of errors described above are exacerbated at high redshifts. High redshift galaxies are usually faint, therefore with large photometric errors, and as the color/redshift space has a very extended range in  $z$ , the degeneracies are more likely; in addition the template incompleteness is worsened as there are few or no empirical spectra with which compare the template library.

The accuracy of any photometric redshift technique is usually established by contrasting its output with a sample of galaxies with spectroscopic redshifts. It should be kept in mind, though, that the results of this comparison may be misleading, as the available spectroscopic samples are almost ‘by definition’ especially well suited for photometric redshift estimation: relatively bright (and thus with small photometric errors) and often filling a privileged niche in the color-redshift space, far from degeneracies (e.g. Lyman-break galaxies). Thus, it is risky to extrapolate the accuracy reached by current methods as estimated from spectroscopic samples (and this also applies to BPZ) to fainter magnitudes. This is especially true for the training set methods, which deliberately minimize the difference between the spectroscopic and photometric redshifts.

### 3. Maximum likelihood (ML) redshift estimates

Photometric redshift techniques based on template fitting look for the best estimate of a galaxy redshift from the comparison of its measured fluxes in  $n_c + 1$  filters  $\{f_\alpha\}$ ,  $\alpha = 0, n_c$ , with a set of  $n_T$  template spectra which try to represent the different morphological types, and which have fluxes  $f_{T\alpha}(z)$ . These methods find their estimate  $z_{ML}$  by maximizing the likelihood  $\mathcal{L}$  (or equivalently minimizing  $\chi^2$ ) over all the possible values of the redshift  $z$ , the templates  $T$  and the normalization constant  $a_0$ .

$$-\log(\mathcal{L}) + \text{const} \propto \chi^2(z, T, a_0) = \sum_{\alpha} \frac{(f_\alpha - a_0 f_{T\alpha})^2}{2\sigma_{f_\alpha}^2} \quad (5)$$

Since the normalization constant  $a_0$  is considered a free parameter, the only information relevant to the redshift determination is contained in the ratios among the fluxes  $\{f_\alpha\}$ , that is, in the galaxy colors.

The definition of the likelihood in eq. (5) is not convenient for applying Bayesian methods as it depends on a normalization parameter  $a_0$ , which is not convenient to define useful priors either theoretically or from previous observations. Here we prefer to normalize the total fluxes in each band by the flux in a ‘base’ filter, e.g. the one corresponding to the band in which the galaxy sample was selected and is considered to be complete. Then the ‘colors’  $C = \{c_i\}$ , are defined as  $c_i = f_i/f_0$   $i = 1, n_c$ , where  $f_0$  is the base flux. The exact way in which the colors are defined is not relevant, other combinations of filters are equally valid. Hereinafter the magnitude  $m_0$  (corresponding to the flux  $f_0$ ) will be used instead of  $f_0$  in the expressions for the priors. And so, assuming that the magnitude errors  $\{\sigma_{f_\alpha}\}$  are gaussianly distributed, the likelihood can be defined as

$$\mathcal{L}(T, z) = \frac{1}{\sqrt{(2\pi)^{n_c} |\Lambda_{ij}|}} e^{-\frac{\chi^2}{2}} \quad (6)$$

where

$$\chi^2 = \sum_{i,j} \Lambda_{ij}^{-1} [c_i - c_{Ti}(z)] [c_j - c_{Tj}(z)] \quad (7)$$

and the matrix of moments  $\Lambda_{ij} \equiv <\sigma_{c_i}\sigma_{c_j}>$  can be expressed as

$$\Lambda_{ij} = f_0^{-4} (f_i f_j \sigma_{f_0}^2 + f_0^2 \delta_{ij} \sigma_{f_i} \sigma_{f_j}) \quad (8)$$

By normalizing by  $f_0$  instead of  $a_0$ , one reduces the computational burden as it is not necessary to maximize over  $f_0$ , which is already the ‘maximum likelihood’ estimate for the value of the galaxy flux in that filter. It is obvious that this assumes that the errors in the

colors are gaussian, which in general is not the case, even if the flux errors are. Fortunately, the practical test performed below (Sec. 5) shows that there is little change between the results using both likelihood definitions (see fig. 3a).

#### 4. Bayesian photometric redshifts (BPZ)

Within the framework of Bayesian probability, the problem of photometric redshift estimation can be posed as finding the probability  $p(z|D, I)$ , i.e., the probability of a galaxy having redshift  $z$  given the data  $D = \{C, m_0\}$ , and the prior information  $I$ . As it was mentioned in the introduction, Bayesian theory states that *all* the probabilities are conditional; they do not represent frequencies, but states of knowledge about hypothesis, and therefore always depend on other data or information (for a detailed discussion of this and many other interesting issues see Jaynes, 1998). The prior information  $I$  is an ample term which in general should include any knowledge that may be relevant to the hypothesis under consideration and is not already included in the data  $C, m_0$ . Note that in Bayesian probability the relationship between the prior and posterior information is *logical*; it does not have to be temporal or even causal. For instance, data from a new observation may be included as prior information to estimate the photometric redshifts of an old data set. Although some authors recommend that the ‘ $|I$ ’ should not be dropped from the expressions of probability (as a remainder of the fact that all probabilities are conditional and especially to avoid confusions when two probabilities based on different prior informations are considered as equal), here the rule of simplifying the mathematical notation whenever there is no danger of confusion will be followed, and from now  $p(z)$  will stand for  $p(z|I)$ ,  $p(D|z)$  for  $p(D|z, I)$  etc.

As a trivial example of the application of Bayes’s theorem, let’s consider the case if which there is only one template and the likelihood  $\mathcal{L}$  only depends on the redshift  $z$ . Then, applying Bayes theorem

$$p(z|C, m_0) = \frac{p(z|m_0)p(C|z)}{p(C)} \propto p(z|m_0)p(C|z) \quad (9)$$

The expression  $p(C|z) \equiv \mathcal{L}$  is simply the likelihood: the probability of observing the colors  $C$  if the galaxy has redshift  $z$  (it is assumed for simplicity that  $\mathcal{L}$  only depends on the redshift and morphological type, and not on  $m_0$ ) The probability  $p(C)$  is a normalization constant, and usually there is no need to calculate it.

The first factor, the *prior* probability  $p(z|m_0)$ , is the redshift distribution for galaxies with magnitude  $m_0$ . This function allows to include information as the existence of upper

or lower limits on the galaxy redshifts, the presence of a cluster in the field, etc. The effect of the prior  $p(z|m_0)$  on the estimation depends on how informative it is. It is obvious that for a constant prior (all redshifts equally likely *a priori*) the estimate obtained from eq. (9) will exactly coincide with the ML result. This is also roughly true if the prior is ‘smooth’ enough and does not present significant structure. However, in other cases, values of the redshifts which are considered very improbable from the prior information would be “discriminated”; they must fit the data much better than any other redshift in order to be selected.

Note that in rigor, one should write the prior in eq. (9) as

$$p(z|m_0) = \int dm_0 p(\hat{m}_0) p(m_0|\hat{m}_0) p(z|\hat{m}_0) \quad (10)$$

where  $\hat{m}_0$  is the ‘true’ value of the observed magnitude  $m_0$ ,  $p(\hat{m}_0)$  is proportional to the number counts as a function of the magnitude  $m_0$  and  $p(m_0|\hat{m}_0) \propto \exp[-(m_0 - \hat{m}_0)^2/2\sigma_{m_0}^2]$ , i.e, the probability of observing  $m_0$  if the true magnitude is  $\hat{m}_0$ . The above convolution accounts for the uncertainty in the value of the magnitude  $m_0$ , which has the effect of slightly ‘blurring’ and biasing the redshift distribution  $p(z|m_0)$ . To simplify our exposition this effect would not be considered hereinafter, and just  $p(z|m_0)$  and its equivalents will be used.

#### 4.1. Bayesian Marginalization

It may seem from eq. 9 (and unfortunately it is quite a widespread misconception) that the only difference between Bayesian and ML estimates is the introduction of a prior, in this case,  $p(z|m_0)$ . However, there is more to Bayesian probability than just priors.

The galaxy under consideration may belong to different morphological types represented by a set of  $n_T$  templates. This set is considered to be *exhaustive*, i.e including all possible types, and *exclusive*: the galaxy cannot belong to two types at the same time. In that case, using Bayesian marginalization (eq. 4) the probability  $p(z|D)$  can be ‘expanded’ into a ‘basis’ formed by the hypothesis  $p(z, T|D)$  (the probability of the galaxy redshift being  $z$  *and* the galaxy type being  $T$ ). The sum over all these ‘atomic’ hypothesis will give the total probability  $p(z|D)$ . That is,

$$p(z|C, m_0) = \sum_T p(z, T|C, m_0) \propto \sum_T p(z, T|m_0) p(C|z, T) \quad (11)$$

$p(C|z, T)$  is the likelihood of the data  $C$  given  $z$  and  $T$ . The prior  $p(z, T|m_0)$  may be developed using the product rule. For instance

$$p(z, T|m_0) = p(T|m_0) p(z|T, m_0) \quad (12)$$

where  $p(T|m_0)$  is the galaxy type fraction as a function of magnitude and  $p(z|T, m_0)$  is the redshift distribution for galaxies of a given spectral type and magnitude.

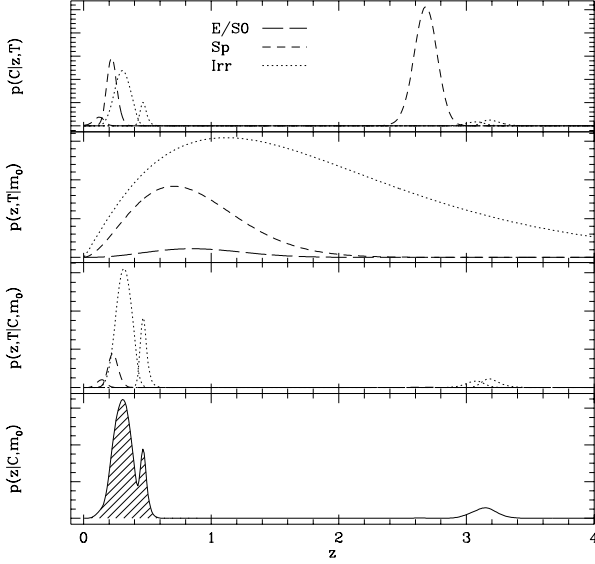


Fig. 2.— An example of the main probability distributions involved in BPZ for a galaxy at  $z = 0.28$  with an Irr spectral type and  $I \approx 26$  to which random photometric noise is added. From top to bottom: a) The likelihood functions  $p(C|z, T)$  for the different templates used in Sec 5. Based on ML, the redshift chosen for this galaxy would be  $z_{ML} = 2.685$  and its spectral type would correspond to a Spiral. b) The prior probabilities  $p(z, T|m_0)$  for each of the spectral types (see text). Note that the probability of finding a Spiral spectral type with  $z > 2.5$  and a magnitude  $I = 26$  is almost negligible. c) The probability distributions  $p(z, T|C, m_0) \propto p(z, T|m_0)p(C|z, T)$ , that is, the likelihoods in the top plot multiplied by the priors. The high redshift peak due to the Spiral has disappeared, although there is still a little chance of the galaxy being at high redshift if it has a Irr spectrum, but the main concentration of probability is now at low redshift. d) The final Bayesian probability  $p(z|C, m_0) = \sum_T p(z, T|C, m_0)$ , which has its maximum at  $z_B = 0.305$ . The shaded area corresponds to the value of  $p_{\Delta z}$ , which estimates the reliability of  $z_B$  and yields a value of  $\approx 0.91$ .

Eq. (11) and fig. 2 clearly illustrate the main differences between the Bayesian and ML methods. ML would just pick the highest maximum over all the  $p(C|z, T)$  as the best redshift estimate, without looking at the plausibility of the corresponding values of  $z$  or  $T$ . On the contrary, Bayesian probability averages all these likelihood functions after weighting them by their prior probabilities  $p(z, T|m_0)$ . In this way the estimation is not affected by

spurious likelihood peaks caused by noise as it is shown in fig. 2 (see also the results of Sec. 5). Of course that in an ideal situation with perfect, noiseless observations (and a nondegenerate template space, i.e, only one  $C$  for each  $(z, T)$  pair) the results obtained with ML and Bayesian inference would be the same.

Instead of a discrete set of templates, the comparison library may contain spectra which are a function of continuous parameters. For instance, synthetic spectral templates depend on the metallicity  $Z$ , the dust content, the star formation history, etc. Even starting from a set of a few templates, they may be expanded using the principal component analysis (PCA) technique (Sodré & Cuevas 1997). In general, if the spectra are characterized by  $n_A$  possible parameters  $A = \{a_1 \dots a_{n_A}\}$  (which may be physical characteristics of the models or just PCA coefficients), the probability of  $z$  given  $F$  can be expressed as

$$p(z|C, m_0) = \int dA p(z, A|C, m_0) \propto \int dA p(z, A|m_0) p(C|z, A) \quad (13)$$

## 4.2. ‘Bookmaker’ odds

Sometimes, instead of finding a ‘point’ estimate for a galaxy redshift, one needs to establish if that redshift belongs within a certain interval. For instance, the problem may be to determine whether the galaxy has  $z > z_t$ , where  $z_t$  is a given threshold, or whether its redshift falls within a given  $z \pm \Delta z$ , e.g. in the selection of cluster members or background galaxies for lensing studies.

As an example, let’s consider the classification of galaxies into the background-foreground classes with respect to a certain redshift threshold  $z_{th}$ . One must choose between the hypothesis  $H_{th} = \{z > z_{th}\}$  and its opposite,  $\bar{H}_{th} = \{z < z_{th}\}$ . The corresponding probabilities may be written as

$$P(H_{th}|D) = \int_0^{z_{th}} dz p(z|D) \quad (14)$$

And

$$P(\bar{H}_{th}|D) = \int_{z_{th}}^{\infty} dz p(z|D) \quad (15)$$

The (‘bookmaker’) odds of hypothesis  $H_{th}$  are defined as the probability of  $H_{th}$  being true over the probability of  $H_{th}$  being false (Jaynes 1998)

$$O(H_{th}|D) = \frac{P(H_{th}|D)}{P(\bar{H}_{th}|D)} \quad (16)$$

When  $O(H_{th}|D) \approx 1$ , there is not enough information to choose between both hypothesis. A galaxy is considered to have  $z > z_{th}$  if  $O(H_{th}|D) > O_d$ , where  $O_d$  is a certain decision

threshold. There are no fixed rules to choose the value of  $O_d$ , and the most appropriate value depends on the task at hand; for instance, to be really sure that no foreground galaxy has sneaked into the background sample,  $O_d$  would have to be high, but if the main goal is selecting all the background galaxies and one does not mind including some foreground ones, then  $O_d$  would be lower, etc. Basically this is a problem concerning decision theory.

In the same way, the cluster galaxies can be selected by choosing a redshift threshold  $\Delta z$  which defines whether a galaxy belongs to the cluster. The corresponding hypothesis would be  $H_c = \{|z - z_c| < \Delta z\}$ .

$$P(H_c|D) = \int_{z_c - \Delta z}^{z_c + \Delta z} dz p(z|D) \quad (17)$$

And

$$P(\bar{H}_c|D) = \int_0^{z_c - \Delta z} dz p(z|D) + \int_{z_c + \Delta z}^{\infty} dz p(z|D) \quad (18)$$

Similarly, the odds of  $H_c$  are defined as

$$O(H_c|D) = \frac{P(H_c|D)}{P(\bar{H}_c|D)} \quad (19)$$

### 4.3. Prior calibration

In those cases where the prior information is vague and does not allow to choose a definite expression prior probability, Bayesian inference offers the possibility of “calibrating” the prior, if needed using the very data sample under consideration.

Let's suppose that the distribution  $p(z, T, m_0)$  is parametrized using  $n_\lambda$  continuous parameters  $\lambda$ . They may be the coefficients of a polynomial fit, a wavelet expansion, etc. In that case, including  $\lambda$  in eq. (11), the probability can be written as

$$p(z|C, m_0) = \int d\lambda \sum_T p(z, T, \lambda|C, m_0) \propto \int d\lambda p(\lambda) \sum_T p(z, T, m_0|\lambda) p(C|z, T) \quad (20)$$

where  $p(\lambda)$  is the prior probability of  $\lambda$ , and  $p(z, T, m_0|\lambda)$  is the prior probability of  $z, T$  and  $m_0$  as a function of the parameters  $\lambda$ . The latter have not been included in the likelihood expression since  $C$  is totally determined once the values of  $z$  and  $T$  are known.

Now let's suppose that the galaxy belongs to a sample containing  $n_g$  galaxies. Each  $j$ -th galaxy has a ‘base’ magnitude  $m_{0j}$  and colors  $C_j$ . The sets  $\mathbf{C} \equiv \{C_j\}$  and  $\mathbf{m}_0 \equiv \{m_{0j}\}$ ,  $j = 1, n_g$  contain respectively the colors and magnitudes of all the galaxies

in the sample. Then, the probability of the  $i$ –th galaxy having redshift  $z_i$  given the full sample data  $\mathbf{C}$  and  $\mathbf{m}_0$  can be written as

$$p(z_i|\mathbf{C}, \mathbf{m}_0) = \int d\lambda \sum_T p(z_i, T, \lambda | C_i, m_{0i}, \mathbf{C}', \mathbf{m}'_0) \quad (21)$$

The sets  $\mathbf{C}' \equiv \{C_j\}$  and  $\mathbf{m}'_0 \equiv \{m_{0j}\}$ ,  $j = 1, n_g, j \neq i$  are identical to  $\mathbf{C}$  and  $\mathbf{m}_0$  except for the exclusion of the data  $C_i$  and  $m_{0i}$ . Applying Bayes' theorem, the product rule and simplifying

$$p(z_i|\mathbf{C}, \mathbf{m}_0) \propto \int d\lambda p(\lambda|\mathbf{C}', \mathbf{m}'_0) \sum_T p(z_i, T, m_{0i}|\lambda) p(C|z_i, T) \quad (22)$$

where as before it has been considered that the likelihood of  $C_i$  only depends on  $z_i, T$  and that the probability of  $z_i$  and  $T$  only depend on  $\mathbf{C}'$  and  $\mathbf{m}'_0$  through  $\lambda$ . The expression to which we arrived is very similar to eq. (20) only that now the shape of the prior is estimated from the data  $\mathbf{C}', \mathbf{m}'_0$ . This means that even if one starts with a very sketchy idea about the shape of the prior, the very galaxy sample under study can be used to determine the value of the parameters  $\lambda$ , and thus to provide a more accurate estimate of the individual galaxy characteristics. Assuming that the data  $\mathbf{C}'$  (as well as  $\mathbf{m}_0$ ) are independent among themselves

$$p(\lambda|\mathbf{C}', \mathbf{m}'_0) \propto p(\lambda)p(\mathbf{C}', \mathbf{m}'_0|\lambda) = p(\lambda) \prod_{j,j \neq i} p(C_j, m_{0j}|\lambda) \quad (23)$$

where

$$p(C_j, m_{0j}|\lambda) = \int dz_j \sum_{T_j} p(z_j, T_j, C_j, m_{0j}|\lambda) \propto \int dz_j \sum_{T_j} p(z_j, T_j, m_{0j}|\lambda) p(C|z_j, T_j) \quad (24)$$

If the number of galaxies in our sample is large enough, it can be reasonably assumed that the prior probability  $p(\lambda|\mathbf{C}', \mathbf{m}'_0)$  will not change appreciably with the inclusion of the data  $C_i, m_{0i}$  belonging to a single galaxy. In that case, a time-saving approximation is to use as a prior the probability  $p(\lambda|\mathbf{C}, \mathbf{m}_0)$ , calculated using the whole data set, instead of finding  $p(\lambda|\mathbf{C}', \mathbf{m}'_0)$  for each galaxy. In addition, it should be noted that  $p(\lambda|\mathbf{C}, \mathbf{m}_0)$  represents the Bayesian estimate of the parameters which define the shape of the redshift distribution (see fig. 10).

#### 4.4. Including spectroscopical information

In some cases spectroscopical redshifts  $\{z_{si}\}$  are available for a fraction of the galaxy sample. It is straightforward to include them in the prior calibration procedure described above, using a delta–function likelihood weighted by the probability of the galaxy belonging

to a morphological type, as it is done to determine the priors in Sec 5. This gives the spectroscopic subsample a (deserved) larger weight in the determination of the redshift and morphological priors in comparison with the rest of the galaxies, at least within a certain color and magnitude region, but, unlike what happens with the training set method, the information contained in the rest of the sample is not thrown away.

If nevertheless one wants to follow the training set approach and use only the spectroscopic sample, it is easy to develop a Bayesian variant of this method. As before, the goal is to find an expression of the sort  $p(z|C, m_0)$ , which would give us the redshift probability for a galaxy given its colors and magnitude. If the color/magnitude/redshift multidimensional surface  $z = z(C, m_0)$  were infinitely thin, the probability would just be  $p(z|C, m_0) \equiv \delta(z(C, m_0))$ , where  $\delta(\dots)$  is a delta-function. But in the real world there is always some scatter around the surface defined by  $z(C, m_0)$  (even without taking into account the color/redshift degeneracies), and it is therefore more appropriate to describe  $p(z|C, m_0)$  as e.g. a gaussian of width  $\sigma z$  centered on each point of the surface  $z(C, m_0)$ . Let's assume that all the parameters which define the shape of this relationship, together with  $\sigma z$  are included in the set  $\lambda_z$ . Using the prior calibration method introduced above, the probability distribution for these parameters  $p(\lambda_z|D_T)$  can be determined from the training set  $D_T \equiv \{z_{si}, C_i, m_{0i}\}$ .

$$p(\lambda_z|D_T) \propto p(\lambda_z) \prod_i p(z_{si}|C_i, m_{0i}, \lambda_z) \quad (25)$$

The expression for the redshift probability of a galaxy with colors  $C$  and  $m_0$  would then be

$$p(z|C, m_0) = \int d\lambda_z p(\lambda_z|D_T) p(z|C, m_0, \lambda_z) \quad (26)$$

The redshift probability obtained from eq. (26) is compatible with the one obtained in eq. (11) using the SED-fitting procedure. Therefore it is possible to combine them in a same expression. As an approximation, let's suppose that both of them are given equal weights, then

$$p(z|C, m_0) \propto \sum_T p(z, T|m_0) p(C|z, T) + \int d\lambda_z p(\lambda_z|D) p(z|C, m, \sigma_z, \lambda_z) \quad (27)$$

In fact, due to the above described redundancy between the SED-fitting method and the training set method (Sec. 2), it would be more appropriate to combine both probabilities using weights which would take these redundancies into account in a consistent way, roughly using eq.(26) at brighter magnitudes, where the galaxies are well studied spectroscopically and leaving eq.(11) for fainter magnitudes. The exploration of this combined, training

set/SED-fitting approach will be left for a future paper, and in the practical tests performed below the followed procedure uses the SED-fitting likelihood.

## 5. A practical test for BPZ

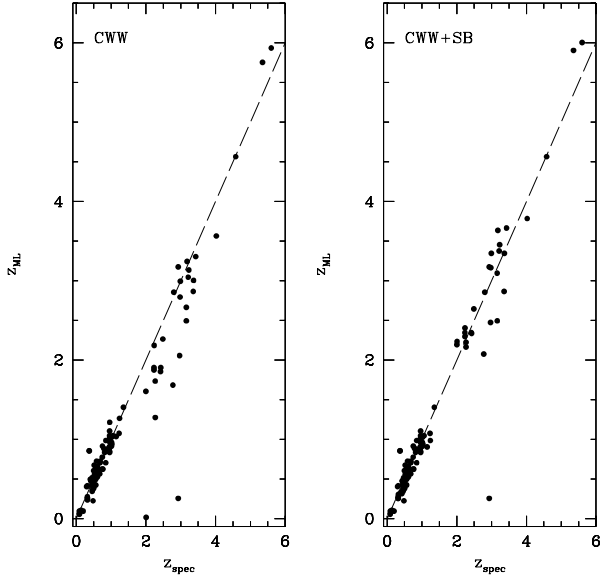


Fig. 3.— a) To the left, the photometric redshifts obtained by applying our ML algorithm to the HDF spectroscopic sample using a template library which contains only the four CWW main types, E/SO, Sbc, Scd and Irr. These results are very similar to those of Fernández-Soto, Lanzetta & Yahil, 1998. b) The right plot shows the significant improvement (without using BPZ yet) obtained by just including two of the Kinney et al. 1996 spectra of starburst galaxies, SB2 and SB3, in the template set. One of the outliers disappears, the ‘sagging’ or systematic offset between  $1.5 < z < 3.5$  is eliminated and the general scatter of the relationship decreases from  $\Delta z/(1 + z_{\text{spec}}) = 0.13$  to  $\Delta z/(1 + z_{\text{spec}}) = 0.10$ .

The Hubble Deep Field (HDF; Williams et al. 1996) has become *the* benchmark in the development of photometric redshift techniques. In this section BPZ will be applied to the HDF and its performance contrasted with the results obtained with the standard ‘frequentist’ (in the Bayesian terminology) method, the procedure usually applied to the HDF (Gwyn & Hartwick 1996, Lanzetta, Yahil & Fernández-Soto 1996, Sawicki, Lin, & Yee 1997, etc.). The photometry used for the HDF is that of Fernández-Soto, Lanzetta & Yahil 1998, which, in addition to magnitudes in the four HDF filters includes JHK magnitudes

from the observations of Dickinson et al. 1998.  $I_{814}$  is chosen as the base magnitude. The colors are defined as described in Sec. 3.

The template library was selected after several tests with the HDF subsample which has spectroscopic redshifts (108 galaxies), spanning the range  $z < 6$ . The set of spectra which worked best is similar to that used by Sawicki, Lin, & Yee 1997. It contains four Coleman, Wu, & Weedman 1980 templates (E/S0, Sbc, Scd, Irr), that is the same spectral types used by Fernández-Soto, Lanzetta & Yahil 1998, plus the spectra of 2 starbursting galaxies from Kinney et al. 1996 (Sawicki, Lin, & Yee 1997 used two very blue SEDs from GISSEL). All the spectra were extended to the UV using a linear extrapolation and a cutoff at 912Å, and to the near-IR using GISSEL synthetic templates. The spectra are corrected for intergalactic absorption following Madau 1995.

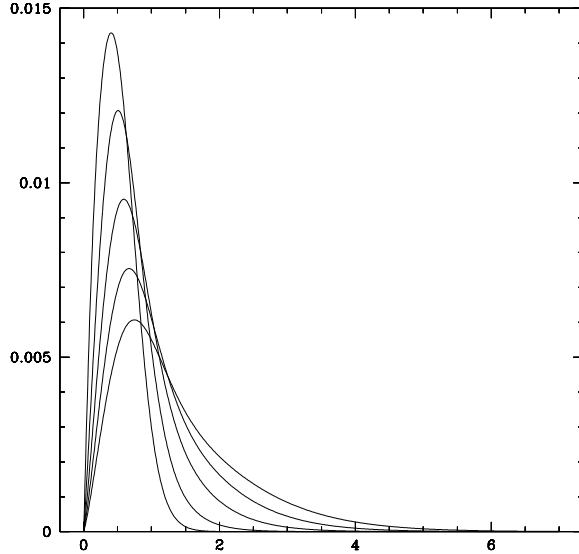


Fig. 4.— The prior in redshift  $p(z|m_0)$  estimated from the HDF data using the prior calibration procedure described in Sec 4., for different values of the magnitude  $m_0$  ( $I_{814} = 21$  to  $I_{814} = 28$ )

It could seem in principle that a synthetic template set which takes (at least tentatively) into account galaxy evolution is more appropriate than ‘frozen’ template library obtained at low redshift and then extrapolated to very high redshifts. However, as Yee 1998 has convincingly shown, the extended CWL set offers much better results than the GISSEL synthetic models Bruzual & Charlot 1993. I have also tried to use the RVF set of spectra and the agreement with the spectroscopic redshifts is considerably worse than using the empirical template set. And if the synthetic models do not work well within the magnitude

range corresponding to the HDF spectroscopic sample is relatively bright, there is little reason to suppose that their performance will improve at fainter magnitudes.

However, even working with empirical templates, it is important to be sure that the template library is complete enough. Fig. 3 illustrates the effects of template incompleteness in the redshift estimation. The left plot displays the results obtained using ML (Sec 3) redshift estimation using only the four CWW templates (this plot is very similar to the  $z_{phot} - z_{spec}$  diagram shown in Fernández-Soto, Lanzetta & Yahil 1998, which confirms the validity of the expression for the likelihood introduced in Sec 3). On the right, the results obtained also using ML (no BPZ yet) but including two more templates, SB2 and SB3 from Kinney et al. 1996. It can be seen that the new templates almost do not affect the low redshift range, but the changes at  $z > 2$  are quite dramatic, the ‘sagging’ of the CWW–only diagram disappears and the general scatter of the diagram decreases by 20%. This shows how important it is to include enough galaxy types in the template library. No matter how sophisticated the statistical treatment is, it will do little to improve the results obtained with a deficient template set.

The first step in the application of BPZ is choosing the shape of the priors. Due to the depth of the HDF there is little previous information about the redshift priors, so this is a good example in which the prior calibration procedure described in Sec 4 has to be applied. It will be assumed that the early types (E/S0) and spirals (Sbc, Scd) have a spectral type prior (eq. 12) of the form

$$p(T|m_0) = f_t e^{-k_t(m_0 - 20)} \quad (28)$$

with  $t = 1$  for early types and  $t = 2$  for spirals. The irregulars (the remaining three templates;  $t = 3$ ) complete the galaxy mix. The fraction of early types at  $I = 20$  is assumed to be  $f_1 = 35\%$  and that of spirals  $f_2 = 50\%$ . The parameters  $k_1$  and  $k_2$  are left as free. Based on the result from redshift surveys the following shape for the redshift prior has been chosen:

$$p(z|T, m_0) \propto z^{\alpha_t} \exp\left\{-\left[\frac{z}{z_{mt}(m_0)}\right]^{\alpha_t}\right\} \quad (29)$$

where

$$z_{mt}(m_0) = z_{0t} + k_{mt}(m_0 - 20) \quad (30)$$

and  $\alpha_t$ ,  $z_{0t}$  and  $k_t$  are considered free parameters. In total, 11 parameters have to be determined using the calibration procedure. For those objects with spectroscopic redshifts, a ‘delta-function’ located at the spectroscopic redshift of the galaxy has been used instead of the likelihood  $p(C|z, T)$ . Table 1 shows the values of the ‘best’ values of the parameters in eq. (29,30) found by maximizing the probability in eq. (26) using the subroutine *amoeba* (Press et al. 1992). The errors roughly indicate the parameter range which encloses 66% of the probability. The values of the parameters in eq. (28) are  $k1 = 0.47 \pm 0.02$  and

$k2 = 0.165 \pm 0.01$ . The prior in redshift  $p(z|m_0)$  can obviously be found by summing over the ‘nuisance’ parameter (Jaynes 1998), in this case  $T$ :

$$p(z|m_0) = \sum_T p(T|m_0)p(z|T, m_0) \quad (31)$$

Fig. 4 plots this prior for different magnitudes.

With the priors thus found, one can proceed with the redshift estimation using eq. (20). Here the multiplication by the probability distribution  $p(\lambda)$  and the integration over  $d\lambda$  will be skipped. As it can be seen from Table 1, the uncertainties in the parameters are rather small and it is obvious that the results would not change appreciably, so the additional computational effort of performing a 11-dimensional integral is not justified.

There are several options to convert the continuous probability  $p(z|C, m_0)$  to a point estimate of the ‘best’ redshift  $z_B$ . Here the ‘mode’ of the final probability is chosen, although taking the ‘median’ value of  $z$ , corresponding to 50% of the cumulative probability, or even the ‘average’  $\langle z \rangle \equiv \int dz z p(z|C, m_0)$  is also valid.

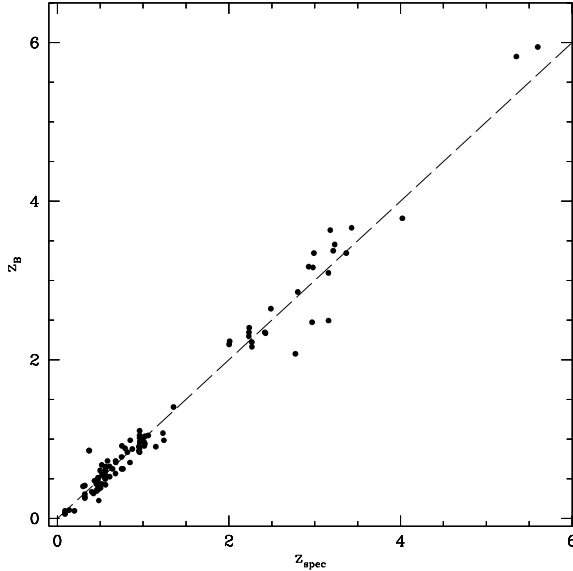


Fig. 5.— The photometric redshifts obtained with BPZ plotted against the spectroscopic redshifts. The differences with fig. 3b are the elimination of 3 galaxies with  $p_{\Delta z} < 0.99$  (see text). This removes the only outlier present in fig. 3b. The rms scatter around the continuous line is  $\Delta z_B/(1 + z_B) = 0.08$ .

It was mentioned in sec 4 that bayesian probability offers a way to characterize the accuracy of the redshift estimation using the odds or a similar indicator, for instance by

analogy with the gaussian distribution a ‘ $1\sigma$ ’ error may be defined using a interval with contains 66% of the integral of  $p(z|C, m_0)$  around  $z_B$ , etc. Here it has been chosen as an indicator of the redshift reliability the quantity  $p_{\Delta z}$ , the probability of  $|z - z_B| < \Delta z$ , where  $z$  is the galaxy redshift. In this way, when the value of  $p_{\Delta z}$  is low, we are warned that the redshift prediction is unreliable. As it will be shown below,  $p_{\Delta z}$  is extremely efficient in picking out galaxies with ‘catastrophic errors’ in their redshifts. The photometric redshifts resulting from applying BPZ to the spectroscopic sample are plotted in fig. 5. Galaxies with a probability  $p_{\Delta z} < 0.99$  (there are three of them) have been discarded, where  $\Delta z$  is chosen to be  $0.2 \times (1 + z)$ , to take into account that the uncertainty grows with the redshift of the galaxies.

It is evident from fig. 5 that the agreement is very good at all redshifts. The residuals  $\Delta z_B = z_B - z_{spec}$  have  $\langle \Delta z_B \rangle = 0.002$ . If  $\Delta z_B$  is divided by a factor  $(1 + z_{spec})$ , as suggested in Fernández-Soto, Lanzetta & Yahil 1998, the rms of the quantity  $\Delta z_B/(1 + z_B)$  is only 0.08. There are no appreciable systematic effects in the residuals. One of the three objects discarded because of their having  $p_{\Delta z} < 0.99$  is the only clear outlier in our ML estimation, with  $z_{BPZ} = 0.245$  and  $z_{spec} = 2.93$  (see fig. 3b), evidence of the usefulness of  $p_{\Delta z}$  to generate a reliable sample.

From the comparison of fig. 3b with fig. 5, it may seem that, apart from the exclusion of the outlier, there is not much profit in applying BPZ with respect to ML. This is not surprising in the particular case of the HDF spectroscopic sample, which is formed mostly by galaxies either very bright or occupying privileged regions in the color space. The corresponding likelihood peaks are thus rather sharp, and little affected by smooth prior probabilities.

To illustrate the effectiveness of BPZ under worse than ideal conditions, the photometric redshifts for the spectroscopic sample are estimated again using ML and BPZ but restricting the color information to the UBV $I$  HST filters. The results are plotted in fig. 6. The ML redshift diagram displays 5 ‘catastrophic errors’ ( $\Delta z \gtrsim 1$ ). Note that these are the same kind of errors pointed out by Ellis 1997 in the first HDF photometric redshifts estimations. BPZ with a  $p_{\Delta z} > 0.99$  threshold (which eliminates a total of 7 galaxies) totally eliminates those outliers. This is a clear example of the capabilities of BPZ (combined with an adequate template set) to obtain reliable photometric redshift estimates. Note that even using near-IR colors, the ML estimates shown in fig. 3 presented outliers. This shows that applying BPZ to UV-only data may yield results more reliable than those obtained with ML including near-IR information! Although of course no more accurate; the scatter of fig. 3b, once the outliers are removed is  $\Delta z \approx 0.18$ , whereas fig. 6b has a scatter of  $\Delta z \approx 0.24$ , which incidentally is approximately the scatter of fig. 3a.

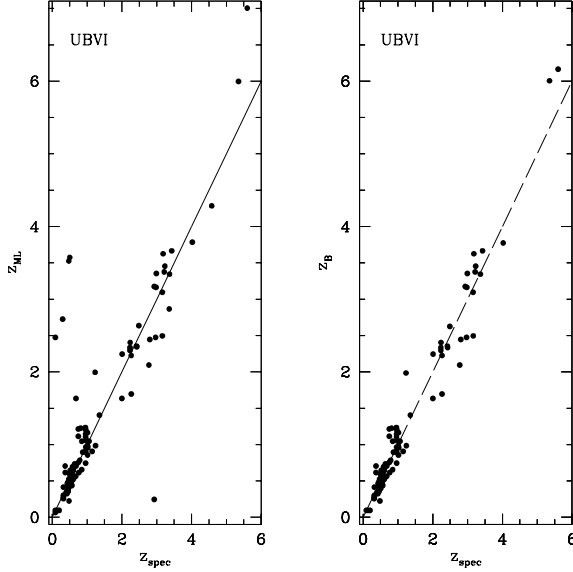


Fig. 6.— a) The left plot shows the results of applying ML to the HDF spectroscopic sample using only the four HST bands. Compare with fig. 3b, which uses also the near IR photometry of Dickinson et al. 1998. The rms of the diagram is increased, and there are several outliers. b) The right plot shows how applying BPZ with a threshold  $p_{\Delta z} > 0.99$  leaves the remaining 101 objects (93.5% of the total) virtually free of outliers. It is noteworthy that these results are totally comparable or even better (as there are no outliers) than those obtained in fig. 3a, in which the near-IR magnitudes were included in the estimation.

Another obvious way of testing the efficiency of BPZ is with a simulated sample. The latter can be generated using the procedure described in Fernández-Soto, Lanzetta & Yahil 1998. Each galaxy in the HDF is assigned a redshift and type using ML (this is done deliberately to avoid biasing the test towards BPZ) and then a mock catalog is created containing the colors corresponding to the best fitting redshifts and templates. To represent the photometric errors present in observations, a random photometric noise of the same amplitude as the photometric error is added to each object. Fig. 7b shows the ML estimated redshifts for the mock catalog ( $I < 28$ ) against the ‘true’ redshifts; although in general the agreement is not bad (as could be expected) there are a large number of outliers (10%), whose positions illustrate the main source of color/redshift degeneracies: high  $z$  galaxies which are erroneously assigned  $z \lesssim 1$  redshifts and vice versa. This shortcoming of the ML method is analyzed in detail in Fernández-Soto, Lanzetta & Yahil 1998. In contrast, fig. 7a shows the results of applying BPZ with a threshold of  $p_{\Delta z} > 0.9$ . This eliminates 20% of the initial sample (almost half of which have catastrophically wrong redshifts), but

the number of outliers is reduced to a remarkable 1%.

Is it possible to define some ‘reliability estimator’, similar to  $p_{\Delta z}$  within the ML framework? The obvious choice seems to be  $\chi^2$ . Fig. 8b plots the value of  $\chi^2$  vs. the ML redshift error for the mock catalog. It is clear that  $\chi^2$  is almost useless to pick out the outliers. The dashed line marks the upper 25% quartile in  $\chi^2$ ; most of the outliers are below it, at smaller  $\chi^2$  values. In stark contrast, fig. 8a plots the errors in the BPZ redshifts *vs.* the values of  $p_{\Delta z}$ . The lower 25% quartile, under the dashed line, contains practically all the outliers. By setting an appropriate threshold one can virtually eliminate the ‘catastrophic errors’.

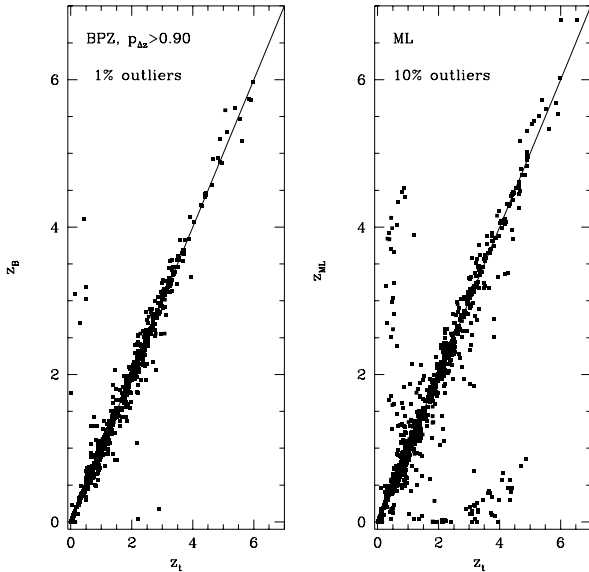


Fig. 7.— a) To the left, the photometric redshifts  $z_B$  estimated using BPZ for the  $I < 28$  HDF mock catalog, plotted against the ‘true’ redshifts  $z_t$  (see text). A threshold of  $p_{\Delta z} > 0.90$ , which eliminates 20% of the objects has been applied. b) The right plot shows the results obtained applying ML to the same mock sample. The fraction of outliers is 10%.

Fig. 9 shows the numbers of galaxies above a given  $p_{\Delta z}$  threshold in the HDF as a function of magnitude and redshifts. It shows how risky it is to estimate photometric redshifts using ML for faint,  $I \gtrsim 27$  objects; the fraction of objects with possible catastrophic errors grows steadily with magnitude.

There is one caveat regarding the use of  $p_{\Delta z}$  or similar quantities as a reliability estimator. They provide a safety check against the color/redshift degeneracies, since basically they tell us if there are other probability peaks comparable to the highest one,

but they cannot protect us from template incompleteness. If the template library does not contain any spectra similar to the one corresponding to the galaxy, there is no indicator able to warn us about the unreliability of the prediction. Because of this, no matter how sophisticated the statistical methods become, it is fundamental to have a good template set, which contains—even if only approximately—all the possible galaxy types present in the sample.

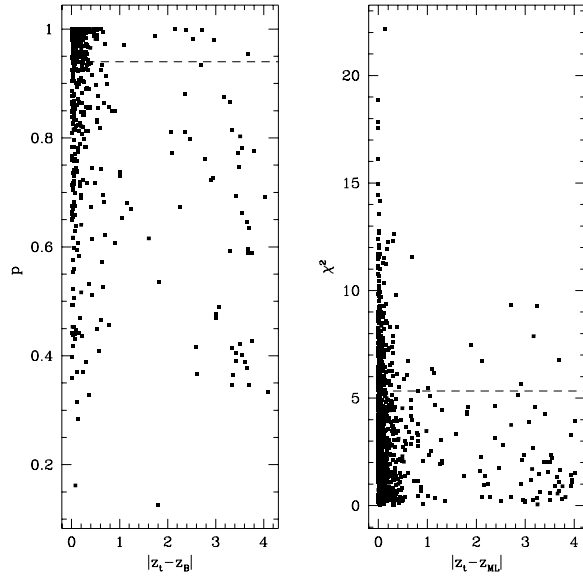


Fig. 8.— a) On the left, the probability  $p_{\Delta z}$  plotted against the absolute value of the difference between the ‘true’ redshift ( $z_t$ ) and the one estimated using BPZ ( $z_B$ ) for the mock sample described in Sec. 5. The higher the value of  $p_{\Delta z}$ , the more reliable the redshift should be. The dashed line shows the 25% low quartile in the value of  $p_{\Delta z}$ . Most of the outliers are at low values of  $p_{\Delta z}$ , what allows to eliminate them by setting a suitable threshold on  $p_{\Delta z}$  (see text and fig. 7) b) The right plot shows that it is not possible to do something similar using ML redshifts and  $\chi^2$  as an estimator. The value of  $\chi^2$  of the best ML fit is plotted against the error in the ML redshift estimation  $|z_t - z_{ML}|$ . The dotted line shows the 25% high quartile in the values of  $\chi^2$ . One would expect that low values of  $\chi^2$  (and therefore better fits) would correspond to more reliable redshifts, but this obviously is not the case. This is not surprising: the outliers in this figure are all due to color/redshifts degeneracies as the one displayed in fig. 1, which may give an extremely good fit to the colors  $C$ , but a totally wrong redshift.

Finally, fig. 10 shows the redshift distributions for the HDF galaxies with  $I < 27$ . No objects have been removed on the basis of  $p_{\Delta z}$ , so the values of the histogram bins should

be taken with care. The overplotted continuous curves are the distributions used as priors and which simultaneously are the Bayesian fits to the final redshift distributions. The results obtained from the HDF will be analyzed in more detail, using a revised photometry, in a forthcoming paper.

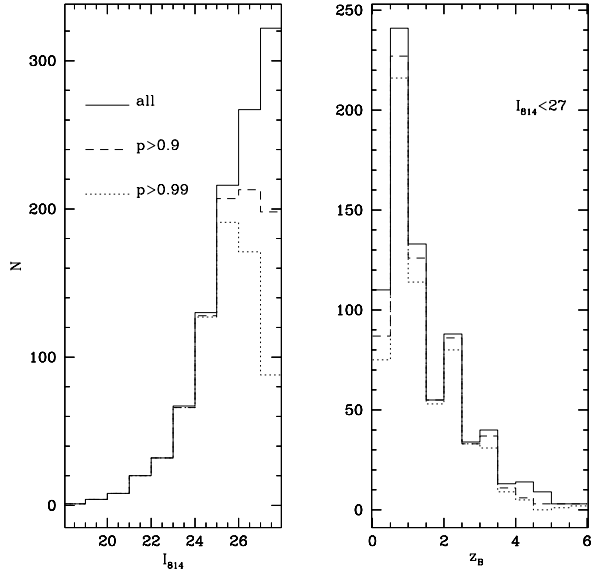


Fig. 9.— a) On the left, histograms showing the number of galaxies over  $p_{\Delta z}$  thresholds of 0.90 and 0.99 as a function of magnitude. It can be seen that the reliability of the photometric redshift estimation quickly degrades with the magnitude. b) The same as a) but as a function of redshift.

## 6. Applications

As we argue above, the use of BPZ for photometric redshift estimation offers obvious advantages over standard ML techniques. However, quite often obtaining photometric redshifts is not an end in itself, but an intermediate step towards measuring other quantities, like the evolution of the star formation rate (Connolly et al. 1997), the galaxy–galaxy correlation function (Connolly, Szalay, & Brunner 1998, Miralles & Pelló 1998), galaxy or cluster mass distributions (Hudson et al. 1998), etc. The usual procedure consists in obtaining photometric redshifts for all the galaxies in the sample, using ML or the training set method, and then work with them as if these estimates were accurate, reliable spectroscopic redshifts. The results of the previous sections alert us to the dangers inherent in that approach, as it hardly takes into account the uncertainties involved in photometric

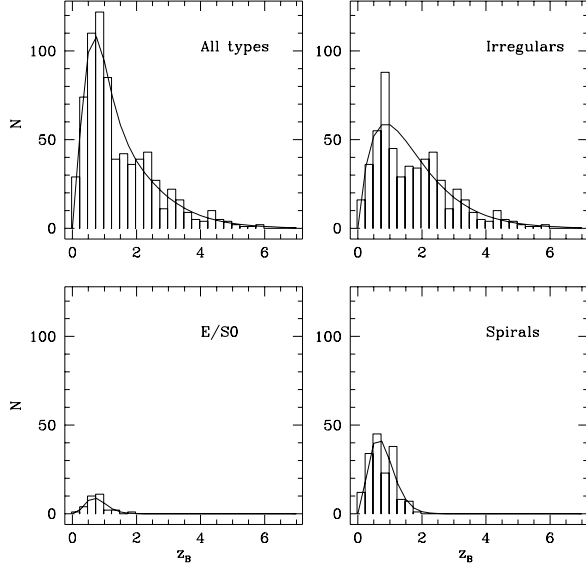


Fig. 10.— The  $z_B$  redshift distributions for the  $I < 27$  HDF galaxies divided by spectral types. The solid lines represent the corresponding  $p(z, T)$  distributions estimated using the prior calibration method described in the text.

redshift estimation. In contrast, within the Bayesian framework there is no need to work with the discrete, point-like ‘best’ redshift estimates. The whole redshift probability distribution can be taken into account, so that the uncertainties in the redshift estimation are accounted for in the final result. To illustrate this point, let’s outline how BPZ can be applied to several problems which use photometric redshift estimation.

### 6.1. Spectral properties of a galaxy population

If, instead of working with a discrete set of templates, one uses a spectral library whose templates depend of parameters as the metallicity, the star-formation history, initial mass function, etc., represented by  $A$  in Sec 4, it is obvious from equation (13) that the same technique used to estimate the redshift can be applied to estimate any of the parameters  $A$  which characterize the galaxy spectrum. For instance, let’s suppose that one want to estimate the parameter  $a_i$ . Then defining  $A' = \{a_j\}, j \neq i$ , we have

$$p(a_i|C, m_0) = \int dz \int dA' p(a_i, z, A'|C, m_0) \propto \int dz \int dA' p(a_i, z, A'|m_0) p(C|z, A) \quad (32)$$

That is, the likelihoods  $p(C|z, A)$  and the weights  $p(a_i, z, A') \equiv p(z, A)$  are the same ones used for the redshift estimation (eq. 13), only that now the integration is performed over the variables  $z$  and  $A'$  instead of  $A$ . In this way, depending on the template library which is being used, one can estimate galaxy characteristics as the metallicity, dust content, etc. An important advantage of this method over ML is that the estimates of the parameter  $a_i$  automatically include the uncertainty of the redshift estimation, which is reflected in the final value of  $p(a_i|C, m_0)$ . Besides, by integrating the probability over all the parameters  $A'$ , one precisely includes the uncertainties caused by possible parameter degeneracies in the final result for  $a_i$ . It should also be noted that as many of the results obtained in this paper, this method can be almost straightforwardly applied to spectroscopical observations; one has only to modify the likelihood expression which compares the observed fluxes with the spectral template. The rest of the formalism remains practically identical.

## 6.2. Galaxy Clusters: member identification

One frequent application of photometric redshift techniques is the study of galaxy cluster fields. The goals may be the selection of cluster galaxies to characterize their properties, especially at high redshifts, or the identification of distant, background galaxies to be used in gravitational lensing analysis (Benítez & Broadhurst 1998). BPZ offers an effective way of dealing with such problems.

To simplify the problem, the effects of gravitational lensing on the background galaxies (magnification, number counts depletion, etc.) will be neglected (see however the next subsection). Let's suppose that we already have an estimate of the projected surface density of cluster galaxies (which can roughly be obtained without any photometric redshifts, just from the number counts surface distribution)  $n_c(m_0, \vec{r})$ , where  $\vec{r}$  is the position with respect to the cluster center. The surface density of 'field', non-cluster galaxies is represented by  $n_f(m_0)$ . For each galaxy in the sample we know its magnitude and colors  $m_0, C$  and also its position  $\vec{r}$ , which is now a relevant parameter in the redshift estimation. Following eq. (11) we can write

$$p(z|C, m_0, \vec{r}) \propto \sum_T p(z, T|m_0, \vec{r}) p(C|z, T) \quad (33)$$

A dependence on the magnitude (e.g. for the early types cluster sequence) could easily be included in the likelihood  $p(C|z, T)$  if needed. The prior can be divided into the sum of two different terms:

$$p(z, T|m_0, \vec{r}) = p_c(z, T|m_0, \vec{r}) + p_f(z, T|m_0, \vec{r}) \quad (34)$$

where  $p_c$  represents the prior probability of the galaxy belonging to the cluster, whereas  $p_f$  corresponds to the prior probability of the galaxy belonging to the general field population.

The expression for  $p_c$  can be written as

$$p_c(z, T|m_0, \vec{r}) = \frac{n_c(m_0, \vec{r})}{n_c(m_0, \vec{r}) + n_f(m_0)} p_c(T|m_0) g(z_c, \sigma z_c) \quad (35)$$

The probability  $p_c(T|m_0)$  corresponds to the expected galaxy mix fraction in the cluster, which in general will depend on the magnitude and will be different from that of field galaxies. The function  $g(z_c, \sigma z_c)$  is the redshift profile of the cluster; a good approximation could be a gaussian with a width corresponding to the cluster velocity dispersion.

The second prior takes the form

$$p_f(z, T|m_0, \vec{r}) = \frac{n_f(m_0)}{n_c(m_0, \vec{r}) + n_f(m_0)} p_f(T|m_0) p_f(z|T, m_0) \quad (36)$$

which uses the priors for the general field galaxy population (Sec 5). Finally, the hypothesis that the galaxy belongs to the cluster or not can be decided about with the help of a properly defined  $p_{\Delta z}$ , or with the odds introduced in Sec 4.

### 6.2.1. Cluster detection

We have assumed above that the cluster redshift and its galaxy surface density distribution are known. However, in some cases, there is a reasonable suspicion about the presence of a cluster at a certain redshift, but not total certainty, and our goal is to confirm its existence. An example using ML photometric redshift estimation is shown in Pelló et al. 1996. An extreme case with minimal prior information occur in optical cluster surveys, galaxy catalogs covering large areas of the sky are searched for clusters. In those cases there are no previous guesses about the position or redshift of the cluster, and a ‘blind’, automatized search algorithm has to be used (Postman et al. 1996).

The prior expression used in the previous subsection offers a way to build such a searching method. Instead of assuming that the cluster redshift and its surface distribution are known, the redshift can be left as a free parameter  $z_c$  and the expression characterizing the cluster galaxy surface density distribution  $n_c(m_0, \vec{r})$  can be parametrized using the quantities  $\lambda_c$ . For simplicity, let’s suppose that

$$n_c(m_0, \vec{r}) = A_c \phi(m_0, z_c) f(\vec{r}_c, \sigma r_c) \quad (37)$$

where  $A_c$  is the cluster ‘amplitude’,  $\phi(m_0, z_c)$  is the number counts distribution expected for the cluster (which in general will depend on the redshift  $z_c$ ) and  $f(\vec{r}_c, \sigma r_c)$  represents

the cluster profile, centered on  $\vec{r}_c$  and with a scale width of  $\sigma r_c$ . This expression, except for the dependence on the redshift is very similar to that used by Postman et al. 1996 to define their likelihood. Then for a multicolor galaxy sample with data  $\mathbf{m}_0$ ,  $\mathbf{C}$  and  $\vec{\mathbf{r}}$ , the probability

$$p(A_c, \vec{r}_c, \sigma r_c, z_c, \sigma z_c | \mathbf{m}_0, \mathbf{C}, \vec{\mathbf{r}}) \quad (38)$$

can be developed analogously to how it was done in Sec. 4. The probability assigned to the existence of a cluster at a certain redshift and position may be simply defined as  $p(A_c | z_c, r_c) > 0$ .

### 6.3. Cluster lensing

It seems that the most obvious application of BPZ to cluster lensing analysis is the selection of background galaxies with the technique described in the previous subsection in order to apply the standard cluster mass reconstruction techniques (Kaiser & Squires 1993, Broadhurst 1995, Seitz, Schneider, & Bartelmann 1998, Taylor et al. 1998). However, using Bayesian probability it is possible to develop an unified approach which simultaneously considers the lensing and photometric information in an optimal way.

In a simplified fashion, the problem of determining the mass distribution of a galaxy cluster from observables can be stated as finding the probability

$$p(\lambda_M, \lambda_C | \mathbf{e}, \vec{\mathbf{r}}, \mathbf{m}_0, \mathbf{C}, \lambda_G) \quad (39)$$

where  $\lambda_M$  represent the parameters which describe the cluster mass distribution; their number may range from a few, if the cluster is described with a simplified analytical model or as many as wanted if the mass distribution is characterized by e.g. Fourier coefficients (Squires & Kaiser 1996).  $\lambda_C$  represents the cosmological parameters, which sensitively affect the lensing strength. The parameter set  $\lambda_G$  represents the properties of the background galaxy population which affect the lensing, as its redshift distribution, number counts slope, etc. and it is assumed to be known previously. The data  $\mathbf{e}$  correspond to the galaxy ellipticities,  $\vec{\mathbf{r}}$  to their angular positions. As above,  $\mathbf{m}_0, \mathbf{C}$  correspond to their colors and magnitudes. For simplicity, it will be assumed that the cluster and foreground galaxies have been already removed and we are dealing only with the background galaxy population.

Analogous to eq. (23), we can develop eq. (39) as

$$p(\lambda_M, \lambda_C | \mathbf{e}, \vec{\mathbf{r}}, \mathbf{m}_0, \mathbf{C}, \lambda_G) \propto p(\lambda_M)p(\lambda_C) \prod_i^{n_g} \int dz_i p(C_i, m_{0i}, \vec{r}_i, e_i, z_i | \lambda_M, \lambda_C, \lambda_G) \quad (40)$$

where the last factor may be written as

$$p(C_i, m_{0i}, \vec{r}_i, e_i, z_i | \lambda_M, \lambda_C, \lambda_G) \propto p(e_i | z_i, \vec{r}_i, \lambda_M, \lambda_C) p(\vec{r}_i | m_{0i}, \lambda_M, \lambda_C, \lambda_G) p(z_i | C, m_{0i}, \vec{r}_i, \lambda_M, \lambda_C, \lambda_G) \quad (41)$$

The meaning of the three factors on the right side of the equation is the following:  $p(e_i | \dots)$  represents the likelihood of measuring a certain ellipticity  $e_i$  in a galaxy given its redshift, position, etc. The second factor  $p(\vec{r}_i | \dots)$  corresponds to the so called “Broadhurst effect”, the number counts depletion of background galaxies caused by the cluster magnification  $\mu$  (Broadhurst 1995, Benítez & Broadhurst 1998). The last factor,  $p(z_i | \dots)$  is the redshift probability, but including a correction which takes into account that the observed magnitude of a galaxy  $m_0$  is affected by the magnification  $\mu(\vec{r})$ . It is clear that the simplified method outlined here is not the only way of applying Bayesian probability to cluster mass reconstruction. My purpose here is to show that this can be done considering the photometric redshifts in a integrated way with the rest of the information.

#### 6.4. Galaxy evolution and cosmological parameters

As it has been shown in section (4), BPZ can be used to estimate the parameters characterizing the joint magnitude–redshift–morphological type galaxy distribution. For small fields, this distribution may be dominated by local perturbations, and the redshift distribution may be ‘spiky’, as it is observed in redshift surveys of small fields. However, if one were to average over a large number of fields, the resulting distribution would contain important information about galaxy evolution and the fundamental cosmological parameters. Sandage 1961 included galaxy counts as one of the four fundamental tests of observational cosmology, although noting that the number-redshift distribution is in fact more sensitive to the value of  $\Omega_0$ . As Gardner 1998 also notes, the color distribution of the galaxies in a survey hold also much more information about the process of galaxy evolution than the raw number counts. However, quite often the only method of analyzing multicolor observations is just comparing them with the number counts model predictions, or at most, with color distributions. There are several attempts at using photometric redshifts to study global galaxy evolution parameters (e.g. Sawicki, Lin, & Yee 1997, Connolly et al. 1997), but so far there is not an integrated statistical method which would simultaneously considers all the information, magnitudes and colors, contained in the data, and set it against the model predictions.

It is then clear that eq. (23) can be used to estimate these parameters from large enough samples of multicolor data. If it is assumed that all the galaxies belong to a few

morphological types, the joint redshift-magnitude-‘type’ distribution can be written as

$$n(z, m_0, T) \propto \frac{dV(z)}{dz} \phi_T(m_0) \quad (42)$$

where  $V(z)$  is the comoving volume as a function of redshift, which depends on the cosmological parameters  $\Omega_0, \Lambda_0$  and  $H_0$ , and  $\phi_T$  is the Schechter luminosity function for each morphological type  $T$ , where the absolute magnitude  $M_0$  has been substituted by the apparent magnitude  $m_0$  (a transformation which depends on the redshifts, cosmological parameters and morphological type). Schechter’s function also depend on  $M^*$ ,  $\alpha$  and  $\phi^*$ , and on the evolutionary parameters  $\epsilon$ , such as the merging rate, the luminosity evolution, etc. Therefore, the prior probability of  $z, A$  and  $m_0$  depends on the parameters  $\lambda_C = \{\Omega_0, \Lambda_0, H_0\}$ ,  $\lambda_* = \{M^*, \phi^* \alpha\}$  and  $\epsilon$ . As an example, let’s suppose that one wants to estimate  $\epsilon$ , independently of the rest of the parameters, given the data  $\mathbf{D} \equiv \{D_i\} \equiv \{C_i, m_{0i}\}$ . Then

$$p(\epsilon | \mathbf{D}) = \int d\lambda_C d\lambda_* p(\epsilon, \lambda_C, \lambda_* | \mathbf{D}) \quad (43)$$

$$p(\epsilon | \mathbf{D}) \propto \int d\lambda_C d\lambda_* p(\epsilon, \lambda_C, \lambda_*) \prod_i \int dz_i \sum_T p(z_i, T, m_{0i} | \epsilon, \lambda_C, \lambda_*) p(C_i | z_i, T) \quad (44)$$

The prior  $p(z_i, T, m_{0i} | \epsilon, \lambda_C, \lambda_*)$  can be derived from  $n(z, m_0, T)$  in eq. (42). The prior  $p(\epsilon, \lambda_C, \lambda_*)$  allows to include the uncertainties derived from previous observations or theory in the values of these parameters, even when they are strongly correlated among themselves, as in the case of the Schechter function parameters  $\lambda_*$ . The narrower the prior  $p(\epsilon, \lambda_C, \lambda_*)$  is, the less ‘diluted’ the probability of  $\epsilon$  and the more accurate the estimation.

## 7. Conclusions

Despite the remarkable progress of faint galaxy spectroscopical surveys, photometric redshift techniques will become increasingly important in the future. The most frequent approaches, the template-fitting and empirical training set methods, present several problems related which hinder their practical application. Here it is shown that by consistently applying Bayesian probability to photometric redshift estimation, most of those problems are efficiently solved. The use of prior probabilities and Bayesian marginalization allows the inclusion of valuable information as the shape of the redshift distributions or the galaxy type fractions, which is usually ignored by other methods. It is possible to characterize the accuracy of the redshift estimation in a way with no equivalents in other statistical approaches; this property allows to select galaxy samples for which the redshift estimation is extremely reliable. In those cases when the *a priori* information is

insufficient, it is shown how to ‘calibrate’ the prior distributions, using even the data under consideration. In this way it is possible to determine the properties of individual galaxies more accurately and simultaneously estimate their statistical properties in an optimal fashion.

The photometric redshifts obtained for the Hubble Deep Field using optical and near-IR photometry show an excellent agreement with the  $\sim 100$  spectroscopic redshifts published up to date in the interval  $1 < z < 6$ , yielding a rms error  $\Delta z_B/(1 + z_{spec}) = 0.08$  and no outliers. Note that these results, obtained with an empirical set of templates, have not been reached by minimizing the difference between spectroscopic and photometric redshifts (as for empirical training set techniques, which may lead to an overestimation of their precision) and thus offer a reasonable estimate of the predictive capabilities of BPZ. The reliability of the method is also tested by estimating redshifts in the HDF but restricting the color information to the UBVI filters; the results are shown to be more reliable than those obtained with the existing techniques even including the near-IR information.

The Bayesian formalism developed here can be generalized to deal with a wide range of problems which make use of photometric redshifts. Several applications are outlined, e.g. the estimation of individual galaxy characteristics as the metallicity, dust content, etc., or the study of galaxy evolution and the cosmological parameters from large multicolor surveys. Finally, using Bayesian probability it is possible to develop an integrated statistical method for cluster mass reconstruction which simultaneously considers the information provided by gravitational lensing and photometric redshift estimation.

I would like to thank Tom Broadhurst and Rychard Bouwens for careful reading the manuscript and making valuable comments. Thanks also to Alberto Fernández-Soto and collaborators for kindly providing me with the HDF photometry and filter transmissions, and to Brenda Frye for help with the intergalactic absorption correction. The author acknowledges a Basque Government postdoctoral fellowship.

## REFERENCES

Benítez, N. & Broadhurst, T. 1998, in preparation

Bretthorst, L. 1988, Bayesian Spectrum Analysis and Parameter Estimation, Lecture Notes Series, vol. 48, Springer–Verlag

Bretthorst, L. 1990, Journal of Magnetic Resonance, 88, 552

Broadhurst, T. 1995, astro-ph/9511150

Brunner, R. J., Connolly, A. J., Szalay, A. S., & Bershady, M. A. 1997, ApJ, 482, L21

Bruzual A., G. & Charlot, S. 1993, ApJ, 405, 538

Coleman, G. D., Wu, C.-C., & Weedman, D. W. 1980, ApJS, 43, 393

Connolly, A. J., Csabai, I., Szalay, A. S., Koo, D. C., Kron, R. G., & Munn, J. A. 1995, AJ, 110, 2655

Connolly, A. J., Szalay, A. S., Dickinson, M., Subbarao, M. U., & Brunner, R. J. 1997, ApJ, 486, L11

Connolly, A. J., Szalay, A. S., & Brunner, R. J. 1998, ApJ, 499, L125

Dey, A., Spinrad, H., Stern, D., Graham, J. R., & Chaffee, F. H. 1998, ApJ, 498, L93

Dickinson, M. et al. 1998, in preparation

Ellis, R. S. 1997, ARA&A, 35, 389

Franx, M., Illingworth, G. D., Kelson, D. D., Van Dokkum, P. G., & Tran, K.-V. 1997, ApJ, 486, L75

Frye, B., Broadhurst, T. & Benítez, N. 1998, in preparation

Fernández-Soto, A., Lanzetta, K.M. & Yahil, A. 1998, to appear in ApJ, astro-ph/9809126

Gardner, J. P. 1998, PASP, 110, 291

Giallongo, E., D’Odorico, S., Fontana, A., Cristiani, S., Egami, E., Hu, E., & McMahon, R. G. 1998, AJ, 115, 2169

Gwyn, S. D. J. & Hartwick, F. D. A. 1996, ApJ, 468, L77

Hogg, D. W., et al. 1998, AJ, 115, 1418

Hudson, M. J., Gwyn, S. D. J., Dahle, H., & Kaiser, N. 1998, ApJ, 503, 531

E.T. Jaynes, “Probability theory: The logic of science”, to be published in Cambridge University Press. A preliminary version can be obtained from Thomas Loredo’s web page at <http://astrosun.tn.cornell.edu/staff/loredo/bayes/>.

Kaiser, N. & Squires, G. 1993, ApJ, 404, 441

Kinney, A. L., Calzetti, D., Bohlin, R. C., McQuade, K., Storchi-Bergmann, T., & Schmitt, H. R. 1996, *ApJ*, 467, 38

Kodama, T., Bell, E. F. & Caldwell, N. 1998, to appear in *MNRAS*, astro-ph/9806120

Koo, D.C. 1985, *AJ*, 90, 418

Lanzetta, K.M., Yahil, A. & Fernández-Soto, A. 1996, *Nature*, 381, 759

Liu, C. T. & Green, R. F. 1998, *AJ*, 116, 1074

Loredo, T. 1990, in *Maximum Entropy and Bayesian Methods*, Darmouth, Ed. P., Fougere, Kluwer Academic Publishers, p. 81-142

Loredo, T. 1992, in *Statistical Challenges in Modern Astronomy*, ed. E.D. Feigelson and G.J. Babu (New York: Springer-Verlag) pp. 275–297

Madau, P. 1995, *ApJ*, 441, 18

Miralles, J.M. & Pelló, R. 1998, astro-ph/9801062

Pello, R., Miralles, J.M., Le Borgne, J.-F., Picat, J.-P., Soucail, G., & Bruzual, G. 1996, *A&A*, 314, 73

Postman, M., Lubin, L. M., Gunn, J. E., Oke, J.B., Hoessel, J. G., Schneider, D. P., & Christensen, J. A. 1996, *AJ*, 111, 615

Press, W. H., Teukolsky, S. A., Vetterling, W. T., & Flannery, B. P. 1992, *Numerical recipes in FORTRAN. The art of scientific computing*, Cambridge: University Press.

Sandage, A. 1961a, *ApJ*, 133, 355

Sawicki, M. J., Lin, H., & Yee, H. K. C. 1997, *AJ*, 113, 1

Seitz, S., Schneider, P., & Bartelmann, M. 1998, *A&A*, 337, 325

Sodré, L. & Cuevas, H. 1997, *MNRAS*, 287, 137

Squires, G. & Kaiser, N. 1996, *ApJ*, 473, 65

Taylor, A. N., Dye, S., Broadhurst, T. J., Benitez, N., & Van Kampen, E. 1998, *ApJ*, 501, 539

Wang, Y., Bahcall, N. & Turner, E.L. 1998, to appear in *AJ*, astro-ph/9804195

Williams, R. E., et al. 1996, AJ, 112, 1335

Yee, H.K.C. 1998, to appear in the proceedings of the Xth Rencontres de Blois,  
astro-ph/9809347

Table 1. Parameters of the priors  $p(z|T, m_0)$  (see text)

Spectral type	$\alpha_t$	$z_{0t}$	$k_{mt}$
E/S0	$2.26 \pm 0.05$	$0.48 \pm 0.03$	$0.061 \pm 0.06$
Sbc,Scd	$1.71 \pm 0.04$	$0.44 \pm 0.02$	$0.044 \pm 0.002$
Irr	$1.125 \pm 0.015$	$0.038 \pm 0.01$	$0.178 \pm 0.002$